The discharge behaviour of the porous lead electrode in the lead-acid battery. II. Mathematical model

P. EKDUNGE[1]*, D. SIMONSSON[2]

[1]Department of Chemical Technology and [2]Department of Applied Electrochemistry and Corrosion Science,
The Royal Institute of Technology, S-100 44 Stockholm, Sweden

A mathematical model for the porous lead electrode in the lead-acid battery has been derived in order to explain the limited discharge capacity at high rates of discharge. By comparison with experimental discharge curves the model predicts that the discharge process is ended by a coverage of the electro-active surface of lead by lead sulphate, even at current densities around $1000 \, A \, m^{-2}$. Only at concentrations lower than the normal (4–5 M) and very high current densities will depletion of sulphuric acid become a limitation. By using an expression which relates the local maximum utilization of the active material to the time integral of the local current density in a way which resembles the empirical Peukert equation, final lead sulphate distributions can be predicted with a maximum in the centre of the electrode, which is in agreement with measurements.

1. Introduction

In a previous work, the electrode kinetics and the structural changes of the porous lead electrode during discharge were studied experimentally [1]. For the explanation and prediction of the discharge behaviour of the porous lead electrode there is a need for a mathematical model which takes into account the intrinsic electrode kinetics and transport equations as well as the structural changes.

Mathematical models for porous electrodes have been reviewed by Newman and Tiedeman [2]. A mathematical model for the porous lead electrode in the lead-acid cell has earlier been presented by Micka and Roušar [3]. Their model used the exact transport equations for concentrated electrolytes and is based on the assumption that the electrode potential is governed only by Nernst's equation. In a later paper on the modelling of the complete cell [4], the effect of charge transfer overvoltage was also considered by adopting a Tafel slope of 15 mV decade^{-1} according to Kabanov [5].

The aim of the present work is to develop a simple mathematical model for the porous lead electrode in sulphuric acid, which takes into consideration the kinetics of the electrode process, the ionic mass transfer in the pores and the effect of structural changes on the kinetics and the transport parameters.

2. The mathematical model

2.1. Basic assumptions

The mathematical model for the porous lead electrode is a modification of the model developed earlier by Simonsson [6] for the discharge process of the porous lead dioxide electrode.

The porous body is assumed to be macrohomogeneous with the pores completely filled with electrolyte, a solution of sulphuric acid. During discharge an anodic current flows through the matrix–electrolyte interface, according to the electrochemical reaction

$$Pb(s) + HSO_4^- (aq) \rightleftharpoons PbSO_4(s) + H^+(aq) + 2e^- \quad (1)$$
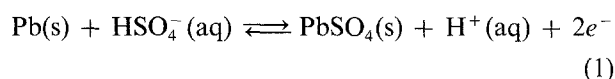
According to this stoichiometry sulphuric acid is consumed, which leads to a concentration gradient in the pores. The lead matrix shrinks, while lead sulphate is formed in the pores. The molar volume of lead sulphate is much higher than that of lead, which results in a decrease in porosity.

To facilitate the analysis, a number of assumptions were made as in [6]. It has thus been assumed that the transport processes in the electrolyte solution can be adequately described by the equations for dilute solution. Also, the sulphuric acid solution is considered as a binary electrolyte of only H^+ and HSO_4^- ions. The equations for the one-dimensional porous lead electrode can then be derived as for the lead dioxide electrode [6]. The coordinate $x = 0$ at the centre of symmetry of the electrode and $x = L$ at the outer surface.

2.2. The effect of structural changes on electrode kinetics and transport rates

It has previously been shown [1] that a relationship between current and charge transfer overvoltage for the porous lead electrode can be described by the kinetic expression

$$\frac{\partial i_e}{\partial x} = \frac{(S_2 J_0)^0 \, (1 - \exp(2\eta')) \, (1 - q/q_d)^m}{(S_2 J_0/j_{lim}^c)^0 - \exp(\alpha_c \eta')} \quad (2)$$

which takes into account the structural changes by

means of the factor $(1 - q/q_d)^m$.

S_2 = specific active surface of lead (m^{-1})

J_0 = exchange current density $(A\,m^{-2})$

i_e = current density in the electrolyte phase $(A\,m^{-2})$

$\eta' = \dfrac{F\eta}{RT}$

η = local overvoltage (V)

j^c_{lim} = limiting current for the cathodic reaction $(A\,m^{-3})$

α_c = cathodic transfer coefficient

The structural changes also affect the effective transport coefficients. During the discharge process lead is converted to lead sulphate, which has a larger molar volume, which leads to a continuous plugging of the pores and decreasing mass transport rates. To take this effect into account, the structural changes were related to the local degree of discharge, which can be calculated from the amount of charge which has been consumed

$$X = \frac{1}{q_0} \int_0^{t'} \frac{\partial i_e}{\partial x}\, dt \qquad (3)$$

where q_0 is the quantity of charge corresponding to the initial amount of lead $(A\,s\,m^{-3})$.

The relation between the local degree of discharge and the local porosity can be expressed as

$$\varepsilon = \varepsilon_0 - k\,(1 - \varepsilon_0)X \qquad (4)$$

where ε_0 = initial porosity, $k = (V_p - V_r)/V_r = 1.67$, the relative difference in molar volume between $PbSO_4$ and Pb. It was shown in [1] that the relationship between effective conductivity, κ, and the porosity can be satisfactorily described by the relation

$$\frac{\kappa}{\kappa_c} = \left(\frac{\varepsilon}{\varepsilon_0}\right)^{1.5} \qquad (5)$$

where κ_c = initial effective conductivity when the sulphuric acid concentration $= c$ $(\Omega^{-1}\,m^{-1})$.

It is assumed that the increasing hindrance for diffusion during discharge, due to structural changes, obeys the same relationship, e.g.

$$D = D_c \left(\frac{\varepsilon}{\varepsilon_0}\right)^{1.5} \qquad (6)$$

where D_c = initial effective diffusion coefficient when the sulphuric acid concentration $= c$ $(m^2\,s^{-1})$.

The rate of decrease in active surface area during discharge is taken into account in Equation 2 by the factor $(1 - q/q_d)^m$, which for $m = 1$ is equivalent to the expression used in [6] for the porous lead dioxide electrode.

The charge output at completed discharge, q_d, varies with the discharge current density even in the absence of diffusion limitations. This can be explained by the fact that with an increasing current density the lead sulphate crystals become more numerous and smaller, which leads to a more rapid coverage of the active lead surface by lead sulphate. In the absence of a theory for this effect, some advantage can be taken

from the empirical Peukert equation, which for galvanostatic discharges relates the time of discharge to the current density

$$i^n t_d = K_a \qquad (7)$$

where i = geometric current density $(A\,m^{-2})$; t_d = time for a complete discharge (s); n and K_a are constants.

For a planar lead electrode, the discharge capacity of which is limited by coverage with lead sulphate crystals, the value of the exponent n is in the range 1.34–1.45 [7].

Since $q_d = it_d$, Equation 7 can be written in the equivalent form

$$q_d = K_a / i^{(n-1)} \qquad (8)$$

This relation can be used together with $q = it$ in the expression for the decreasing specific active surface area

$$S_2 = S_2^0\,(1 - q/q_d)^m = S_2^0\,(1 - i^n t/K_a)^m \qquad (9)$$

where S_2^0 is the initial surface area of lead.

While Equation 9 can be used for a planar electrode at galvanostatic discharges, it should be modified for a porous electrode to account for the local current density $J = (1/S_2^0)(\partial i_e/\partial x)$ instead of the geometric current density i. With a changing current distribution the local current density varies with time even during discharge with a constant geometric current density. The expression for the local active surface area in a porous electrode may therefore be written

$$S_2 = S_2^0\left(1 - \frac{I^n}{K_a'}\int_0^{t'}\left(\frac{\partial i}{\partial z}\right)^n dt\right)^m \qquad (10)$$

where $K_a' = K_a(S_2^0 L)^n$.

2.3. Model equations

The mathematical model derived by Simonsson [6] for the porous lead dioxide electrode can be used also for the porous lead electrode, after correcting for the stoichiometry, kinetics and structural changes. The equations were made dimensionless by the following transformations

$$z = \frac{x}{L}; \quad C = \frac{c}{c_0}; \quad \tau = \frac{D_0 t}{L^2};$$

$$E' = \frac{FE_c}{RT}; \quad i = \frac{i_e}{I}$$

where L = the thickness of one symmetric half of the porous electrode (m); c_0 = the initial concentration of sulphuric acid $(kmol\,m^{-3})$; D_0 = effective diffusion coefficient of sulphuric acid at initial conditions; E_c = the equilibrium electrode potential at the actual concentration of sulphuric acid (V); I = the total geometric current density $(A\,m^{-2})$.

The set of equations which represents the model of

the porous lead electrode then becomes

$$i = a \left(\frac{\varepsilon}{\varepsilon_0}\right)^{1.5} \frac{\kappa_c}{\kappa_0} \left(\frac{\partial E'}{\partial C} \frac{\partial C}{\partial z} + \frac{\partial \eta'}{\partial z}\right)$$

$$- b_0 \frac{(D_1 - D_2)_c}{(D_1 - D_2)_0} \left(\frac{\varepsilon}{\varepsilon_0}\right)^{1.5} \frac{\partial C}{\partial z} \qquad (11)$$

$$\frac{\partial C}{\partial \tau} = (1 - 2t_1) \frac{f}{\varepsilon} \frac{\partial i}{\partial z} + \frac{1}{\varepsilon} \frac{\partial}{\partial z} \left(\left(\frac{\varepsilon}{\varepsilon_0}\right)^{1.5} \frac{D_c}{D_0} \frac{\partial C}{\partial z}\right)$$

$$+ \frac{f}{\varepsilon} c_0 (V_p - V_r) i \frac{\partial C}{\partial z} \qquad (12)$$

$$\frac{\partial i}{\partial z} = g \frac{S_2}{S_2^0} \frac{(1 - \exp(2\eta'))}{\left(\frac{S_2 J_0}{j_{lim}^c}\right)^0 - \exp(\alpha_c \eta')} \qquad (13)$$

$$X = \frac{IL}{D_0 q_0} \int_0^\tau \frac{\partial i}{\partial z} d\tau \qquad (14)$$

t_1 in Equation 12 is the transference number of the hydrogen ion. S_2/S_2^0 in Equation 13 is given by Equation 10.

The dimensionless parameters have the following definitions:

$$a = \frac{\kappa_0 RT}{ILF}$$

$$b_0 = \frac{F(D_1 - D_2)_0 c_0}{IL}$$

$$f = \frac{IL}{2FD_0 c_0}$$

$$g = \frac{(S_2 J_0)^0 L}{I}$$

D_1 and D_2 are ionic diffusivities of H^+ and HSO_4^-, respectively.

At the beginning of discharge the electrode is assumed to be fully charged and the electrolyte concentration in the pores uniform and equal to the concentration in the bulk solution. This gives the following initial conditions

at $t = 0$, $C(z) = 1$ and $X(z) = 0$.

The boundary conditions at the surface of the electrode are

at $z = 1$, $i = 1$ and $C = 1$.

The latter assumes that the mass transfer resistance external to the electrode is negligible. At the plane of symmetry of the electrode the boundary conditions are

$$z = 0: \quad \frac{\partial C}{\partial z} = \frac{\partial \eta'}{\partial z} = \frac{\partial \varepsilon}{\partial z} = 0; \quad i = 0.$$

In the previous paper [1] the values of transport parameters and the kinetic parameters appearing in the model were experimentally determined. Other data which are required in the model were taken from suitable literature sources. The data used in the calculations are summarized in Table 1.

Table 1. Numerical values of the parameters used in the model in the standard case

Parameter	Value	Reference
L	1×10^{-3} m	
c_0	5 M	
ε_0	0.60	
D_0	7.2×10^{-10} m^{2}s^{-1}	
D_c/D_0	$0.706 + 0.294 \times C$	
$(D_1 - D_2)$	$= \frac{D(2 - 1/t_1)}{2(1 - t_1)}$	
κ_0	$23 \Omega^{-1}$m^{-1}	[1]
t_1	$0.8224 - 0.0725 \times C$ $- 0.0302 \times C^2$	[9]
$\frac{\partial E'}{\partial c}$	-4.825	[8]
M_{Pb}	207.2 kg kmol^{-1}	[10]
M_{PbSO_4}	303.25 kg kmol^{-1}	[10]
ϱ_{Pb}	11.34×10^3 kg m^{-3}	[10]
ϱ_{PbSO_4}	6.2×10^3 kg m^{-3}	[10]
$V_p = \frac{M_{PbSO_4}}{\varrho_{PbSO_4}}$	48.9×10^{-3} m^3 kmol^{-1}	
$V_r = \frac{M_{Pb}}{\varrho_{Pb}}$	18.3×10^{-3} m^3 kmol^{-1}	
$q_0 = 2F(1 - \varepsilon_0) \frac{\varrho_{Pb}}{M_{Pb}} \times 0.8$	$= 3.37 \times 10^9$ A s^{-1} m^{-3}	
$k = \frac{1}{V_r}(V_p - V_r)$	1.67	
α_c	0.9	[1]

The difference between the individual ionic diffusivities for the hydrogen ion and the bisulphate ion, respectively, has been calculated by using the relation for the binary diffusion coefficient

$$D = \frac{2D_1 D_2}{D_1 + D_2} \qquad (15)$$

and the relation

$$D_1/D_2 = t_1/t_2 \qquad (16)$$

which for a binary electrolyte follows directly from the definition of transference number and the Nernst–Einstein relation.

Equations 15 and 16 give

$$D_1 - D_2 = \frac{D(2 - 1/t_1)}{2(1 - t_1)} \qquad (17)$$

In order to allow for comparisons with experimental results at 22° C literature data were corrected to this temperature. The variation of conductivity with the concentration of sulphuric acid at 22° C was obtained by interpolation between data for 20 and 25° C, respectively.

The diffusion coefficient was calculated from data at 18° C by means of the Stokes–Einstein relation. Effective diffusion coefficients were obtained from the values in free electrolyte by multiplying by the same correction factor as found for the relation between the measured effective conductivity and data for the conductivity in free electrolyte.

Values of effective diffusion coefficients, effective conductivity and geometric current density are given
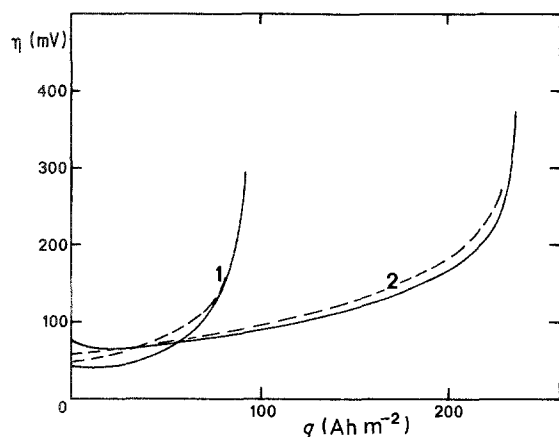
Fig. 1. Comparison of experimental and theoretically predicted galvanostatic discharge curves. $I = 1000\,\mathrm{A\,m^{-2}}$. (1) Electrode without expander. (2) Electrode with 0.08% expander. Solid lines: experimental. Dashed lines: theoretical predictions with

$$K_a' = 4 \times 10^6\ (\mathrm{A\,m^{-2}})^{1.35}\,\mathrm{s},\ (S_2 J_0)^0 = 6 \times 10^5\,\mathrm{A\,m^{-3}}\ \text{and}$$

$$(j_{\mathrm{lim}}^c)^0 = -1.2 \times 10^5\,\mathrm{A\,m^{-3} \qquad (1)}$$

$$K_a' = 11 \times 10^6\ (\mathrm{A\,m^{-2}})^{1.35}\,\mathrm{s},\ (S_2 J_0)^0 = 1.9 \times 10^5\,\mathrm{A\,m^{-3}}\ \text{and}$$

$$(j_{\mathrm{lim}}^c)^0 = -1 \times 10^5\,\mathrm{A\,m^{-3}}. \qquad (2)$$

with respect to the total projected surface of the electrode, including the grid which occupies approximately 20% of this surface. Before being used in the calculations, these values must therefore be multiplied by a factor $1/0.8 = 1.25$ in order to correct for the grid. This correction factor does not affect the parameters a, b_0 and f, since it appears both in the nominator and the denominator in the expressions for these parameters, but it would have a net effect in Equation 14, unless q_0 is also given per unit volume including the grid as in Table 1.

The numerical procedure used to solve the non-linear equation system of the boundary value type was described in [6].

3. Results and discussion

The numerical calculations were carried out for a high rate of discharge with a current density of $1000\,\mathrm{A\,m^{-2}}$.

To judge the relevance of the model a comparison between calculated and experimentally determined discharge curves was made for both an electrode with standard addition of expander and an electrode without organic expander. The value of the exponent n in Equation 10 was taken as 1.35, which is within the range observed on planar lead electrodes by Asai *et al.* [7].

A good first estimate of its value was obtained by using the condition $S_2 = 0$ for $t = t_d$ and the approximation $\partial i/\partial z \approx 1$, i.e. uniform current distribution, in Equation 10. This gives

$$K_a' \approx I^n t_d \qquad (18)$$

The values of the kinetic parameters were taken as obtained in the previous investigations [1]. Calculated and experimental discharge curves are compared in Fig. 1 for both an electrode with and without addition of organic expander. The agreement is fairly good for
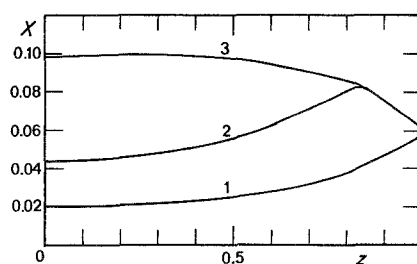

Fig. 2. Predicted lead sulphate distributions along the depth of the electrode without expander after discharge with $1000\,\mathrm{A\,m^{-2}}$ for $100\,\mathrm{s}$ (1), $200\,\mathrm{s}$ (2) and $312\,\mathrm{s}$ ($=100\%$) (3). Parameter values as in Fig. 1.

the electrode with expander, while the deviation is more significant for the electrode without expander. It should be brought to mind that the values of the kinetic parameters have been taken from experiments at a low rate of discharge, where the dissolution-precipitation mechanism should dominate for both types of electrodes, and where the discharge capacities are of the same magnitude [1]. The significantly lower discharge capacity of the electrode without expander as compared to the electrode with expander in Fig. 1 can be explained by a dominating solid-state mechanism in the former electrode.

In that case it is reasonable to expect that the kinetic parameters should have values different from those obtained at a low rate of discharge. In contrast, the electrode with organic expander still operates according to the dissolution-precipitation mechanism even at high discharge current densities, and the kinetic data obtained at a low rate of discharge are still relevant. The value of m has been taken as 1 in Fig. 1. Using $m = 0.5$, as obtained empirically in [1], gives a better agreement between theory and experiment, and actually makes the experimental and calculated discharge curves of the electrode with organic expander coincide completely except for the initial voltage jump. From a physical point of view, however, it is more realistic to assume that $m = 1$ in Equation 9. This value has therefore been chosen as the standard value of m in the calculations.

The calculated lead sulphate distribution across the porous lead electrode is shown indirectly in Figs 2 and 3 as the local extent of discharge as a function of depth. For the electrode without expander the lead sulphate distribution at completed discharge is fairly uniform with a somewhat lower utilization of the outer part of the electrode due to a higher current density, which leads to a more rapid passivation according to Equation 10. The discharge capacity of this electrode is obviously limited by the coverage of the electrode surface by lead sulphate.

The electrode with expander shows a maximum of lead sulphate in the centre of the electrode. This is in agreement with the measured lead sulphate distribution for an electrode with 0.3% expander and for some cross sections of an electrode with 0.08% expander [1], although the measured maximum was more pronounced.

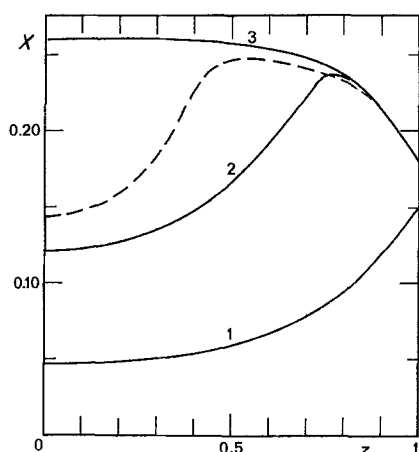The change in concentration of sulphuric acid in the

Fig. 3. Predicted lead sulphate distributions along the depth of the electrode with 0.08% expander after discharge with $1000\,A\,m^{-2}$ for 240 s (1), 580 s (2) and 836 s (= 100%) (3). Parameter values as in Fig. 1. Dashed curve: same electrode with $c_0 = 3\,M$, fully discharged after 700 s.

pores during discharge is very difficult to measure experimentally, but an interpretation of this process is given from the solution of the equations of the model. The mean concentration of sulphuric acid at the end of the discharge can be measured. A comparison of the calculated mean concentration of sulphuric acid at the end of discharge with the measured gives a test of the description of the transport in the pores. The calculated mean concentration was 3.32 M after a discharge with $1000\,A\,m^{-2}$, while the measured [1] was 3.0 M. This rather good agreement is somewhat surprising when taking into consideration that the model is based on the transport equations for dilute solutions. This should be compared with the results from the calculation done by Micka and Roušar [3, 4] based on the exact transport equations, which give a mean concentration of sulphuric acid in the pores at the end of a discharge with $1000\,A\,m^{-3}$ which is higher than 4 M. The calculated concentration profile in the pore electrolyte is shown in Fig. 4 for an initial concentration of 5 and 3 M, respectively. It is evident from this figure that acid depletion limits the discharge capacity in the latter but not in the former case.
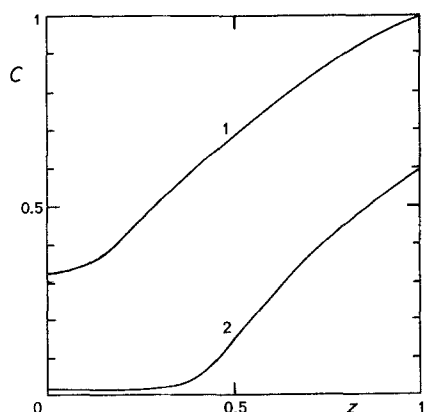
The accuracy of the dilute solution theory can be

Fig. 4. Concentration profile in a lead electrode with 0.08% expander, fully discharged with $1000\,A\,m^{-2}$ in 836 s (1) and 700 s (2), respectively. Initial concentration = 5 M (1) and 3 M (2). Parameter values as in Fig. 1.
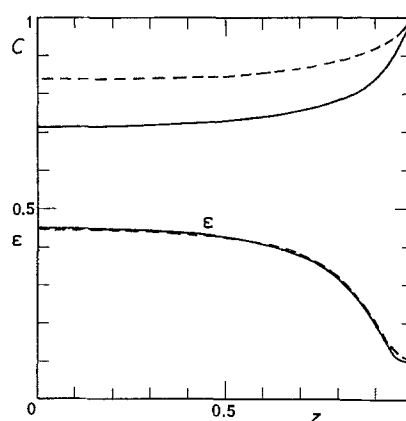

Fig. 5. Calculated distributions of concentration and porosity after a discharge with $1000\,A\,m^{-2}$ for 792 s. Initial porosity = 0.50. Values of input parameters and kinetic equation as in [4]. Solid lines: dilute solution theory; dashed lines: exact mass transport equations, results reported in [4].

determined by a comparison between the results predicted by Micka and Roušar's model [4], using the exact transport equations, and the results predicted by the simplified model used in this paper, when the same input parameters are used. Figure 5 shows that the dilute solution theory predicts a much higher concentration drop in the pore electrolyte. On the other hand, it is also evident that the predicted reaction distribution is not very much affected by the difference in concentration profile. A generalized conclusion would then be that the exactness of the transport equations is of major importance only when the discharge process is limited by the transport rate of sulphuric acid. In this case the discharge capacity is instead limited by structural effects.

According to Micka and Roušar's assumptions the pore entrances become blocked with $PbSO_4$ when the porosity at $x = L$ is equal to 0.1 and at the same time the specific surface area of lead at this location tends to zero. It is obvious from Fig. 5 that these assumptions lead to predicted lead sulphate distributions which are much more non-uniform than those measured experimentally [1]. Also, the assumed least possible value of the porosity corresponds to a maximum active mass utilization, which is much higher than that measured experimentally. It is therefore likely that the discharge capacity is limited by a coverage of the lead surface by lead sulphate rather than a blockage of pore entrances.

Calculations were performed for different concentrations of sulphuric acid to investigate how the concentration influences the discharge capacity. In Fig. 6 the discharge capacity as a function of the electrolyte concentration is illustrated. The calculated capacities are in good agreement with the measured capacities from [1], which are included in Fig. 6 for comparison. For 1–4 M the capacity limiting process is acid depletion, whereas for 5 M it is the isolation of the active lead surface area by lead sulphate.

The mathematical model can be used to predict the behaviour of the lead electrode. The value of different parameters can be varied independently of one another to find the optimum. How the discharge capacity of
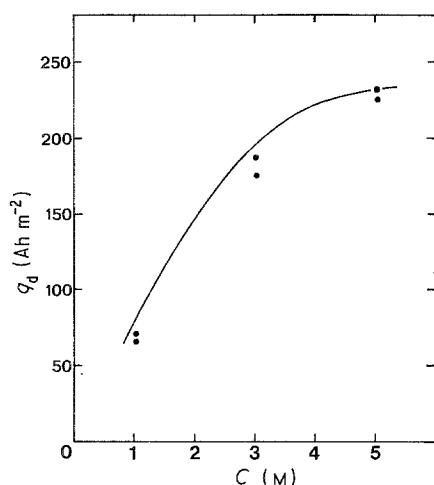
Fig. 6. Discharge capacity at $1000\,A\,m^{-2}$ as a function of sulphuric acid concentration. Solid line: predicted by the model. $K'_a = 11 \times 10^6$. Other parameter values as in Fig. 1. Points: measured discharge capacities according to [1].

Fig. 7. Discharge capacity as a function of K'_a. $n = 1.35$. Other parameter values as in Fig. 1, curve 2. (1) Uniform current distribution; (2) calculated discharge capacity, $c_0 = 5\,M$; (3) calculated discharge capacity, $c_0 = 3\,M$.

the electrode changes with the active surface area can, for instance, be investigated by varying the parameter K'_a, which can be regarded as a measure of the initially available active surface area. In Fig. 7 the discharge capacity is shown as a function of K'_a. In the case of uniform current distribution, Equation 10 is equivalent to Equation 18. The discharge capacity of the porous electrode is $q_d = It_d = K'_a/I^{n-1}$. This relation is shown as a dashed line in Fig. 7.

Discharge capacities calculated with the mathematical model are lower than those calculated for this ideal case of uniform current distribution. This effect is partly due to the non-uniformity of the current distribution and partly due to the limited diffusion rate. The effect of the latter is demonstrated clearly in the difference between the curves for $c_0 = 5\,M$ and $c_0 = 3\,M$, respectively. With $3\,M\ H_2SO_4$ and sufficiently large values of K'_a the discharge capacity will be limited by coverage of the electrode surface by lead sulphate in the outer parts and acid depletion in the inner parts of the electrode, see Figs 3 and 4. Increasing the specific mass utilization (or K'_a) gives a relatively low increase of the discharge capacity, since the utilization of the inner parts cannot be significantly improved because of acid depletion.

For low values of K'_a the discharge capacity is limited by coverage of the lead surface with lead sulphate, and the curves for different acid concentrations coincide in a straight line. The extrapolation of this line corresponds to an electrode with an infinitely high value of the effective diffusion coefficient.

4. Conclusions

The mathematical model for the discharge behaviour of the porous lead electrode presented here is based on rather rough approximations. An exact treatment would require more detailed knowledge about the electrolyte, the electrochemical reaction and structural effects in the porous electrode. Nevertheless, the present model gives a good description of the discharge behaviour of the porous lead electrode. It
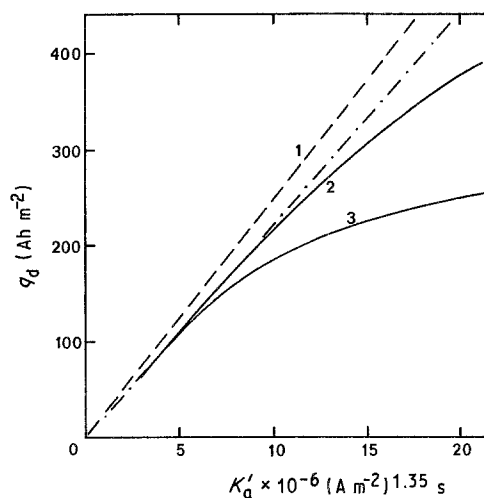
makes it possible to examine the capacity limiting process under different discharge conditions. The calculations presented in this paper show that the discharge capacity even at high current densities (up to $1000\,A\,m^{-2}$) and normal concentration (around $5\,M$) is limited by the coverage of the electrode surface by lead sulphate. Acid depletion is a capacity-limiting process only at sulphuric acid concentrations below or around $3\,M$.

The model can also be used for improvements in the performance of the lead electrode by estimating the relative importance of the various variables. Thus, the reported calculations show that the fractional conversion of the electroactive material is relatively low, about 25% for the electrode with organic expander and only about 10% for the electrode without organic expander. In order to increase the discharge capacity the formation of larger lead sulphate crystals must be further stimulated.

It has also been demonstrated that mathematical modelling of porous electrodes undergoing structural changes, i.e. most battery electrodes, requires a better knowledge of the effects of solid products on the electrode kinetics as a function of current density and concentration of ionic reactants.

References

[1]   P. Ekdunge and D. Simonsson, *J. Appl. Electrochem.* **19** (1989) 127.
[2]   J. Newman and W. Tiedemann, *Am. Inst. Chem. Eng. J.* **21** (1975) 25.
[3]   K. Micka and I. Roušar, *Electrochim. Acta* **19** (1974) 499.
[4]   K. Micka and I. Roušar, *Electrochim. Acta* **21** (1976) 599.
[5]   B. N. Kabanov, in 'Proceeding of Second Conference in Metal Corrosion', Vol. 2 (in Russian) Izd. Akad. Nauk SSSR, Moscow (1943) p. 67.
[6]   D. Simonsson, *J. Appl. Electrochem.* **3** (1973) 261.
[7]   K. Asai, M. Tsubota, K. Yonezu and K. Ando, *J. Power Sources* **7** (1981/82) 73.
[8]   H. Bode, 'Lead–Acid Batteries', Wiley-Interscience, New York (1977).
[9]   K. Micka and I. Roušar, *Electrochim. Acta* **18** (1973) 629.
[10]   'Handbook of Chemistry and Physics', 60th edn, CRC Press (1980).